CORE

Metadata, citation and similar papers at core.ac.uk

Provided by Radboud Repository

Radboud Repository

Radboud University Nijmegen

PDF hosted at the Radboud Repository of the Radboud University Nijmegen

The following full text is a publisher's version.

For additional information about this publication click this link.
http://hdl.handle.net/2066/91960

Please be advised that this information was generated on 2017-12-06 and may be subject to change.

View Article Online / Journal Homepage / Table of Contents for this issue
Dynamic Article Links

Soft Matter

Cite this: *Soft Matter*, 2011, **7**, 7013

www.rsc.org/softmatter

**PAPER**

# Island brushes to control adhesion of water in oil droplets on planar surfaces†

**Khooi Y. Tan,[a] Julien E. Gautrot[a] and Wilhelm T. S. Huck*[ab]**

***Received 16th December 2010, Accepted 3rd May 2011***
**DOI: 10.1039/c0sm01501f**

By using molecular self-assembly and polymer brush chemistry, adhesion of water droplets at solid/oil interfaces could be achieved and modulated by external triggers. Silicon wafers were hydrophobically modified with binary mixed self-assembled layers consisting of fluorinated silanes and atom transfer radical polymerisation (ATRP) initiator silanes, and subsequently grafted with responsive polymers *via* surface-initiated ATRP. Temperature- and pH-responsive adhesion of water in oil droplets occurred on surfaces coated with phase-separated self-assembled layers and grafted with short polymer chains.

## Introduction

Adhesion at solid/liquid interfaces is mainly governed by the surface chemical composition and the surface topography.[1–4] Even on superhydrophobic surfaces with micron- or nano-sized structures (those exhibiting water contact angles higher than 150°), droplets might adhere if the water can partially wet the surfaces. Such wetting causes a transition from a superhydrophobic non-adhering Cassie state to a superhydrophobic adhering Wenzel state. In other words, the contact angle hysteresis ($\theta_{\text{advancing}} - \theta_{\text{receding}}$) increases dramatically, leading to “pinning” of droplets on the surfaces.

Inspired by nature, a plethora of biomimetic high adhesion superhydrophobic surfaces featuring hierarchical micro- and nano-scale structures have been reported, the majority of which studied the adhesion of water or oil droplets at solid/air interfaces.[5] Unlike low adhesion superhydrophobic surfaces exhibiting the classic “lotus effect”,[6] substrates with surface topographies mimicking those of rose petals[7] and gecko feet[8] were able to immobilise water droplets at contact angles greater than 150° and retain the droplets at a tilt angle of 180°. A number of “smart” superhydrophobic surfaces exhibiting switchable adhesion properties at the solid/air interface were fabricated by manipulating the surface chemistry, the surface structure or a combination thereof.[9] Reddy *et al.*[10] demonstrated that adhesion on thermoplastic elastomers could be controlled by modifying the tilt angle of surface microstructures. Other groups used films of hydrophobically modified ZnO nanorods[11] and $TiO_2$ nanotubes[12,13] to alternately switch between the pinning and rolling states upon UV activation and heat deactivation. A reversibly switchable adhesive superhydrophobic surface was also generated by spin-coating a liquid crystal polymer displaying a temperature-dependent transition between a hydrophobic smectic A phase and a hydrophilic isotropic phase on microstructured silicon wafers.[14] More recently, Liu *et al.*[15,16] generated pH- and temperature-responsive adhesive superhydrophobic surfaces by coating anodised aluminium oxide with polymer brushes.

The adhesion of oil or water droplets at solid/liquid interfaces has received relatively less attention. Inspired by the superoleophobic nature of fish scales, Liu *et al.*[17] showed that the adhesion of oil droplets at the solid/water interface could be modulated as a function of the surface roughness: increasing the roughness significantly diminished the adhesion of 1,2-dichloroethane oil droplets on the surface. Chen *et al.*[18] fabricated temperature-responsive adhesive surfaces using poly(*N*-isopropylacrylamide) hydrogels and, interestingly, a *n*-hexane oil droplet spontaneously left the hydrogel/water interface as the environment temperature decreased from 40 to 23 °C.

Here, we designed a new model for switchable adhesive surfaces in water-in-oil emulsions, based on self-organisation and polymer brushes without having to pre-modify the surface roughness, as schematically illustrated in Fig. 1. Droplets adhere to hydrophilic brushes that are grown from phase-separated self-assembled layers in an “archipelago”-like arrangement on an otherwise hydrophobic background. The chemically heterogeneous surface prevents the spreading of droplets, leading to high contact angles. At the same time, the hydrophilic brushes “pin” the droplets, leading to large hysteresis of contact angles. However, this balance is disrupted by the collapse of the brushes in response to external triggers such as temperature and pH. The hydrophobic interactions then dominate the surface and the droplets will retreat from the islands, leading to a low adhesion state.

## Experimental section

### Materials

Di(ethylene glycol) methyl ether methacrylate ($MEO_2MA$), poly (ethylene glycol) methyl ether methacrylate (average $M_n \approx 300$)

---

[a] *Melville Laboratory for Polymer Synthesis, Department of Chemistry, University of Cambridge, Lensfield Road, Cambridge, CB2 1EW, UK. E-mail: wtsh2@cam.ac.uk*

[b] *Radboud University Nijmegen, Institute for Molecules and Materials, Heyendaalseweg 135, 6525 AJ Nijmegen, The Netherlands*

† Electronic supplementary information (ESI) available: See DOI: 10.1039/c0sm01501f

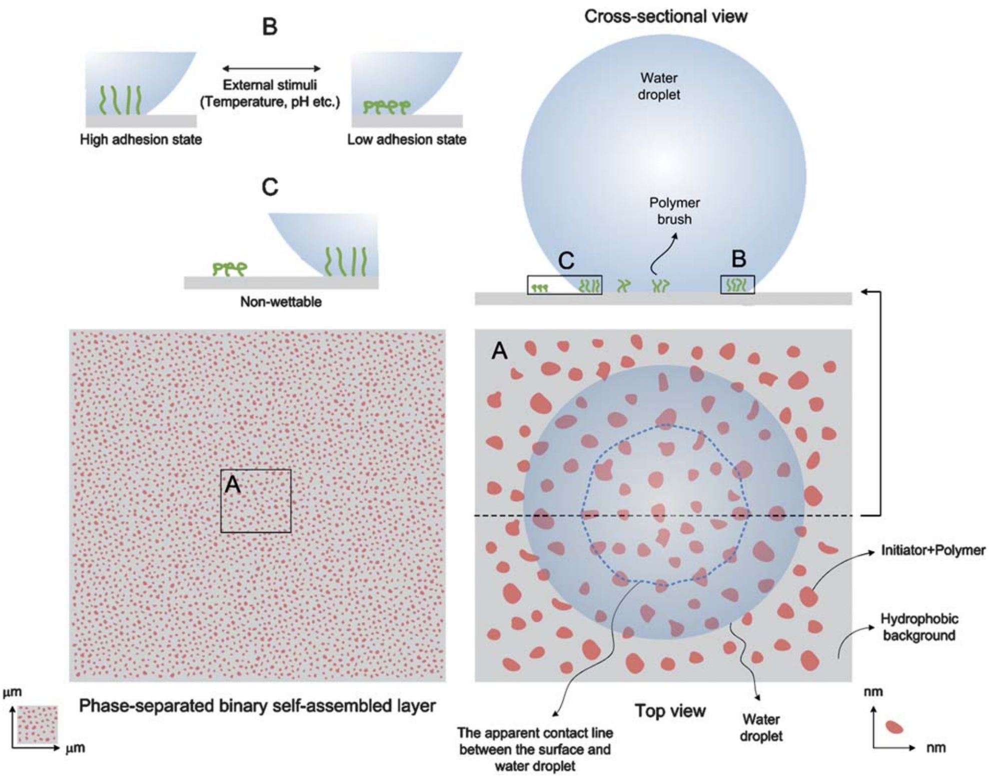

**Fig. 1** Model for switchable adhesive surfaces in water-in-oil emulsions based on self-assembly and polymer brush chemistry. Segregated domains in the phase-separated self-assembled layer are in the nanometre scale. For the purpose of illustration, the size of the water droplet was reduced significantly relative to the size of segregated domains.

(OEGMA), 2-(dimethylamino)ethyl methacrylate (DMAEMA), *N*-isopropylacrylamide (NIPAM), *N*,*N*,*N*′,*N*′′,*N*′′-pentamethyldiethylenetriamine (PMDETA), copper(II) chloride (Cu(II)Cl$_2$), copper(I) bromide (Cu(I)Br) and trichloro(1*H*,1*H*,2*H*,2*H*-perfluorooctyl)silane (PFOTS) were purchased from Aldrich. 2,2′-Dipyridyl (bipy), copper(I) chloride (Cu(I)Cl) and decane (≥99%) were obtained from Sigma-Aldrich. Triethylamine (Et$_3$N) was from Alfa Aesar. All chemicals and solvents were of analytical grades and used as received unless otherwise stated. Cu(I)Cl and Cu(I)Br were kept under vacuum until needed. Et$_3$N was distilled from KOH and stored over molecular sieves (3 Å grade). Purified water with a resistivity of 18.2 MΩ cm (Millipore Synergy system) was used. Anhydrous toluene was withdrawn from a PureSolv solvent purification system (Innovative Technology). The ATRP initiator, 2-bromo-2-methylpropionic acid 3-trichlorosilanylpropyl ester **1**, was synthesised according to a published procedure.[19] Silicon wafers (diameter 100 mm, orientation ⟨100⟩, one side polished) were purchased from Compart Technology and cleaned for 10 min in an air plasma with a forward power of 100 W (Emitech K1050X plasma asher).

## Deposition of ATRP initiator on silicon wafers

A plasma-oxidised silicon wafer was cut into four pieces. Each of these pieces was transferred to a crystallisation dish and immersed in a solution of ATRP initiator **1** (3 μL) and/or PFOTS (volume depended on the desired volume ratio with respect to ATRP initiator **1**), Et$_3$N (3 μL) and anhydrous toluene (50 mL). The crystallisation dish was then covered and left at room temperature (RT) for 18 h. For self-assembled layers containing purely ATRP initiator **1**, the wafer was rinsed with acetone, sonicated in acetone (30 s), rinsed with absolute ethanol and dried under a stream of nitrogen. For self-assembled layers containing PFOTS, the wafer was rinsed with toluene, sonicated successively in toluene, isopropyl alcohol, hexane and acetone (1 min each), rinsed with absolute ethanol and dried under a stream of nitrogen. The coated silicon substrate was kept dry under nitrogen until required.

## Surface-initiated ATRP

Monomers, bipy and/or Cu(II)Cl$_2$ were dissolved in a solvent and degassed by nitrogen bubbling for 30 min with stirring. Cu(I)Cl or Cu(I)Br was added quickly to the mixture and degassing was continued for another 30 min. ATRP initiator-coated silicon substrates (~1 × 1 cm$^2$ each) were transferred into sealed reaction vessels, degassed *via* a minimum of four high-vacuum/nitrogen cycles and left under nitrogen in the vessels. Subsequently, the monomer mixture was transferred *via* degassed syringes to reaction vessels (~5 mL per vessel) and ATRP was allowed to proceed. To terminate polymerisation, substrates were rinsed thoroughly with water and absolute ethanol, and dried under a stream of nitrogen. All steps were performed at RT. Chemicals involved were as follows: for poly(MEO$_2$MA-*co*-OEGMA),[19] MEO$_2$MA 16.94 g (85.5 mmol), OEGMA 2.85 g (9.5 mmol), bipy 782 mg (5.0 mmol), Cu(II)Cl$_2$ 21.5 mg (0.16 mmol), Cu(I)Cl 158.5 mg (1.6 mmol), water/methanol (2 : 1, v/v) 45 mL; for polyNIPAM,[20] NIPAM 1.0 g (8.6 mmol), PMDETA 630 μL (3.0 mmol), Cu(I)Br 95.8 mg (0.67 mmol), water/methanol (3 : 7, v/v) 11.25 mL; for polyDMAEMA,[15] DMAEMA 3.0 mL (17.8 mmol), bipy 183.2 mg (1.2 mmol), Cu(I) Cl 63 mg (0.64 mmol), water/methanol (1 : 1, v/v) 30 mL.

### Surface characterisation

Dry polymer thicknesses were determined *via* an α-SE spectroscopic ellipsometer (J. A. Woollam) with a 632.8 nm laser at an incident angle of 70°. Contact angle measurement was carried out by using a home-built stage with a computer-controlled syringe and a digital camera. Typically, a water droplet (~1.5 μL) was formed at the tip of a needle and brought into contact with a surface. The needle was retracted from the droplet and static contact angle was determined. For polymer thickness and contact angle, measurements were carried out at three different points on each sample and values were presented as averages ± standard deviations. Atomic force microscopy (AFM) was performed for dry samples on a Dimension 3100 microscope (Veeco Instruments) using the tapping mode. Olympus OMCL-AC series silicon probes with a resonant frequency of 300 kHz and a spring constant of 42 N $m^{-1}$ were used. Images were acquired at three different points on a sample at a scan rate of 0.3–0.5 Hz for an area of 10 × 10 $\mu m^2$ and processed using the NanoScope software (Veeco Instruments). The domain size was analysed using the ImageJ software (version 1.44j, "Analyze Particles" option after thresholding) and expressed as averages ± standard errors. For investigating the adhesion behaviour in water-in-oil emulsions, a silicon substrate was placed in a cuvette containing oil and a water droplet (~1.5 μL) was formed at the tip of a needle (21 G, outer diameter 0.81 mm, inner diameter 0.56 mm, blunt tip, Terumo) in the oil. With the aid of an adjustable stage, the silicon substrate was slowly approached to the droplet until they were in contact with each other, and then the substrate was gradually retracted from the droplet. For experiments carried out at temperatures higher than RT, an equilibrium time of 30 min at the desired temperatures was allowed.

## Results and discussion

### Surface characterisation

A range of blends of trichlorosilanes with ATRP initiator **1** (INI) headgroups and hydrophobic fluorine (PFOTS) groups (Fig. 2) were allowed to self-assemble onto silicon wafers.[15] As shown in Fig. 3, the contact angle of INI and/or PFOTS coated surfaces increased linearly with the PFOTS : INI feed ratio from 66 ± 2° (100% INI) to 126 ± 3° (15 : 1 PFOTS : INI) and reached a plateau. In order to ensure the presence of INI in the mixed self-assembled layers, ATRP was carried out on substrates coated with various PFOTS : INI ratios (Fig. 2) and the polymer thickness was determined *via* ellipsometry. For this purpose, a relatively thick layer of polymer is desired because the polymer thickness decreases with the initiator density.[21] As anticipated, dry polymer thicknesses on these substrates exhibited a decreasing profile with respect to the PFOTS : polymer ratio from 66 nm on 100% brush substrates to 6 nm on 40 : 1 PFOTS : polymer substrates (Fig. 3). Note that the polymer chains had equal lengths on all these surfaces as they were synthesised in the same controlled polymerisation steps.[21] On the other hand, contact angles increased systematically with the PFOTS : polymer ratio from 75 ± 5° on 100% brush substrates to 127 ± 6° on 40 : 1 PFOTS : polymer substrates (Fig. 3). These results clearly indicate the successful immobilisation of both INI and PFOTS molecules on the surfaces, and imply that the coating of PFOTS reduced the surface energy of the modified substrates.

AFM was carried out to determine the surface topography of substrates coated with mixed silanes and polymer. A thin layer of polymer is desired to prevent the bridging of polymer chains across the surface which would subsequently mask the surface topography. The ellipsometric dry polymer thicknesses on 100% INI substrates were 10–12 nm. Because the polymer thickness on substrates coated with diluted INI was too thin to be measured, the polymer brush thickness on 100% INI substrates will be used as the reference (hereafter referred to as $h_{\text{ref}}$). AFM images displayed in Fig. 4 reveal the transition from a smooth continuous polymer film (100% polymer) to progressively distributed "dots" (10 : 1, 20 : 1 and 40 : 1 PFOTS : polymer) and eventually well-segregated larger "islands" (60 : 1 PFOTS : polymer). On 40 :1 PFOTS : polymer substrates, the average size of "dots" was 0.020 ± 0.001 $\mu m^2$ whereas on 60 : 1 PFOTS : polymer substrates, the average size of the segregated "islands" was 0.058 ± 0.003 $\mu m^2$ (ESI, Fig. S1† for size distribution). Phase separation occurred most probably due to distinctly dissimilar chemical functionalities of fluorinated and initiator silane molecules, as also reported elsewhere (for example by Fan *et al.*[22]). Both contact angle goniometry and AFM strongly suggest that the segregated and continuous domains in the self-assembled layers were largely composed of INI and PFOTS molecules respectively.

### Temperature-responsive adhesive hydrophobic surfaces in water-in-oil emulsions

In order to obtain responsive adhesive hydrophobic surfaces, two parameters were manipulated: the PFOTS : INI ratio and the length of polymer brushes. The PFOTS : INI ratio enabled us to modulate the size and distance between the adhesive islands, as demonstrated in Fig. 4. The fractional coverage of the hydrophilic regions on the surface will determine the water contact angle, as stated in the Cassie's model of wetting ($\cos \theta_C = f \cos \theta - (1 - f)$ where $f$ is the fraction of the solid/water interface). The length of polymer chains allowed us to control the "strength" of the hydrophilic part of the surface and hence the droplet adhesion. The polymer chains need to be sufficiently long to ensure interactions with the droplet, yet short enough to prevent bridging across islands which would destroy the "archipelago" morphology, as illustrated in Fig. 1.

In the present study, poly($MEO_2MA$-*co*-OEGMA) exhibiting a lower critical solution temperature (LCST) in water was used as the model temperature-responsive polymer. The LCST of this random copolymer, which exhibits low hysteresis between cooling and heating cycles, can be tuned between 26 and 90 °C by varying the monomer composition, and is nearly independent of molar mass, concentration and ionic strength.[23,24] Poly ($MEO_2MA$-*co*-OEGMA) with 90 mol% of $MEO_2MA$ and 10 mol% of OEGMA (average $M_n$ of OEGMA ≈ 300 g $mol^{-1}$) was grafted from silicon substrates. A range of polymer thicknesses ($h_{\text{ref}}$ ≈ 5–66 nm) was obtained by varying the polymerisation

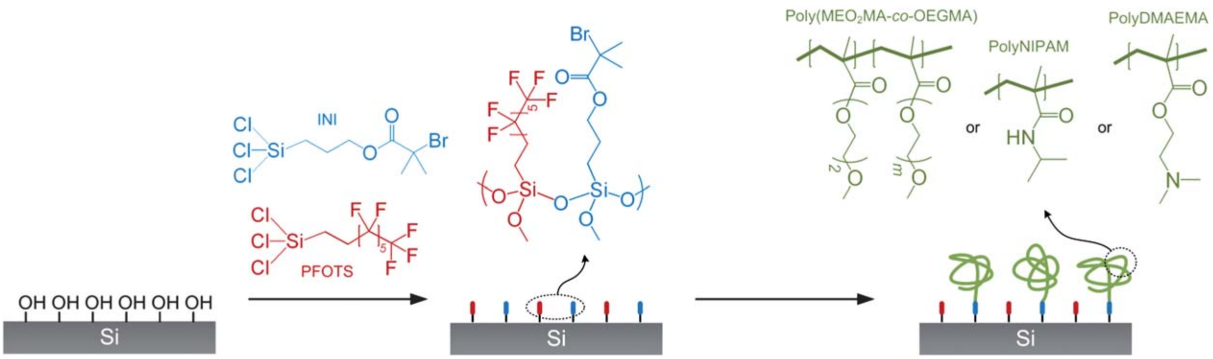

**Fig. 2** Schematic overview of polymer brush formation on silicon substrates *via* self-assembly of INI and/or PFOTS and subsequent surface-initiated ATRP.

time (ATRP 2–120 min) (Fig. S2†). According to Jonas *et al.*,[19,25] poly($MEO_2MA$-*co*-OEGMA) brushes (same $MEO_2MA$ : OEGMA molar ratio but a higher average $M_n$ of OEGMA ≈ 475 g mol$^{-1}$) with a dry thickness of 124 nm on silicon substrates exhibited a LCST of ~40 °C, and thin polymer brushes with dry thicknesses less than 50 nm showed higher LCSTs (*e.g.*, poly-$MEO_2MA$ brushes with thicknesses of 105 and 26 nm exhibited LCSTs of ~32 and ~40 °C respectively).

Decane was used as the continuous oil phase for investigating the adhesion of modified silicon substrates in water-in-oil emulsions. Compared to water in air, contact angles of water in decane at RT on silicon substrates coated with PFOTS : poly($MEO_2MA$-*co*-OEGMA) ($h_{ref}$ ≈ 66 nm) increased significantly (Fig. 5). For substrates coated with 100% poly($MEO_2MA$-*co*-OEGMA) brush, the contact angle increased from 64 ± 11° (water in air) to 110 ± 2° (water in decane). Whilst the contact angle of water in air plateaued at ~113° (30 : 1 PFOTS : poly($MEO_2MA$-*co*-OEGMA)), the contact angle of water in decane increased continuously with the PFOTS : poly($MEO_2MA$-*co*-OEGMA) ratio and reached the maximum at 134 ± 5° (40 : 1 PFOTS : poly($MEO_2MA$-*co*-OEGMA)). The PFOTS-only-coated surfaces became totally non-adhesive to water in decane, as shown in Fig. 5.

Reducing the polymer length from $h_{ref}$ ≈ 66 to 9 nm did not affect the adhesion of water in decane droplets for substrates coated with PFOTS : poly($MEO_2MA$-*co*-OEGMA) (Fig. 5 and

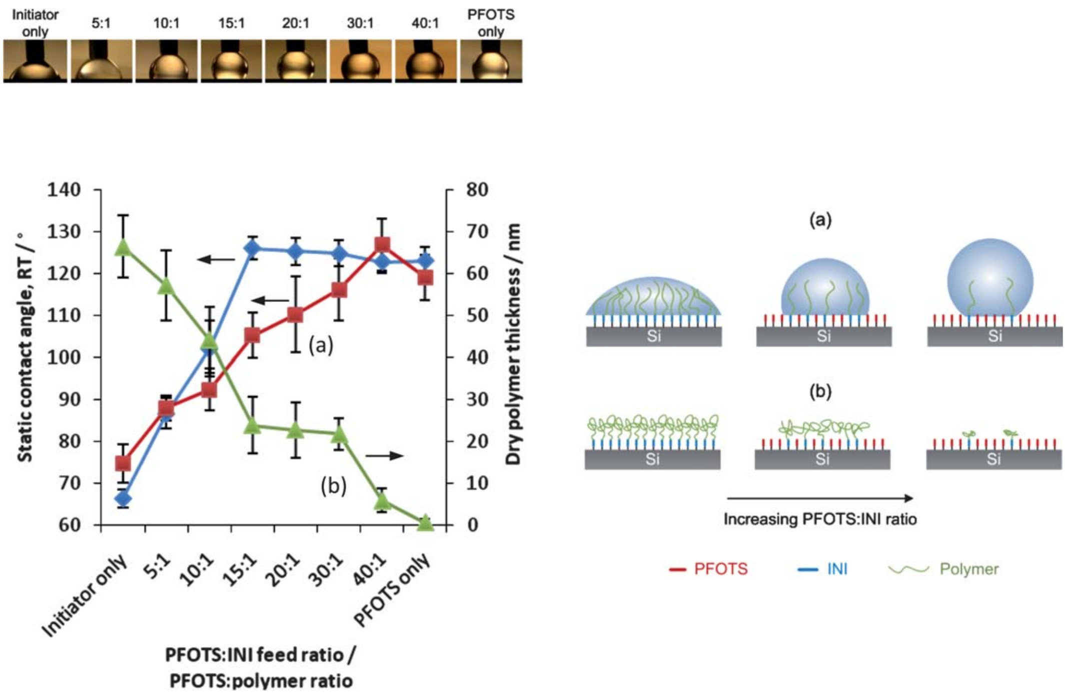

**Fig. 3** Static contact angles of water in air at RT and dry polymer thicknesses on silicon substrates coated with a range of initiator densities. ◆ Static contact angle as a function of PFOTS : INI feed ratio (without polymer) (pictures shown); ■ static contact angle as a function of PFOTS : poly($MEO_2MA$-*co*-OEGMA) ratio. In all cases, the contact angle was determined with the needle remained in contact with the droplet, as shown in the inset pictures. ▲ Ellipsometric dry thickness of poly($MEO_2MA$-*co*-OEGMA) as a function of PFOTS : poly($MEO_2MA$-*co*-OEGMA) ratio grafted on silicon substrates. Graphic representation of the relationship between the PFOTS : polymer ratio and (a) the contact angle and (b) the dry polymer thickness.

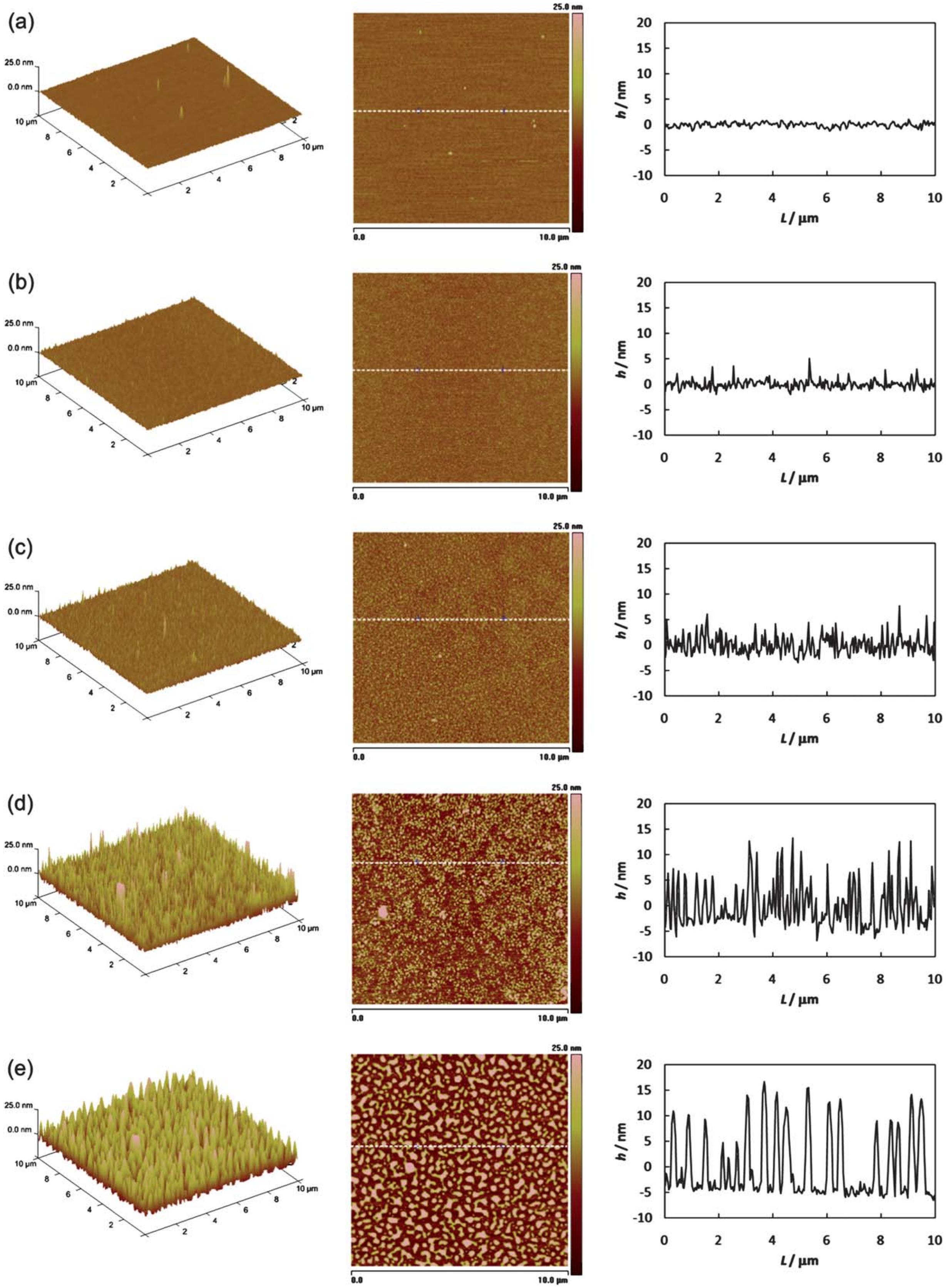

**Fig. 4** AFM images (3D, 2D and cross-sectional views) for silicon substrates coated with various PFOTS : INI ratios and grafted with poly(MEO$_2$MA-*co*-OEGMA) ($h_{\mathrm{ref}} \approx$ 10–12 nm). PFOTS : poly(MEO$_2$MA-*co*-OEGMA) ratio: (a) 100% poly(MEO$_2$MA-*co*-OEGMA) brush, (b) 10 : 1, (c) 20 : 1, (d) 40 : 1 and (e) 60 : 1. Cross-sectional views were taken from 2D images as indicated by the white broken lines.

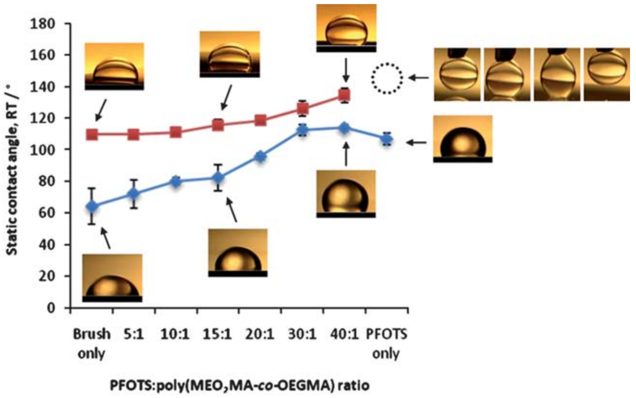

**Fig. 5** Static contact angles of water in air (◆) and water in decane (■) at RT on silicon wafers as a function of the PFOTS : poly(MEO$_2$MA-*co*-OEGMA) ratio ($h_{ref} \approx 66$ nm). Dotted circle signifies that water droplets did not adhere to the surface. Images show that the water in decane droplet did not adhere to a PFOTS-only-coated surface.

6a). In all cases, water droplets adhered to the substrates at RT. However, further reducing the polymer length from $h_{ref} \approx 9$ to 5 nm resulted in non-adhesive substrates (50 : 1 and 55 : 1 PFOTS : poly(MEO$_2$MA-*co*-OEGMA)) (Fig. 6b). This phenomenon indicates the important relationship between the polymer chain length and surface adhesion of these substrates. It suggests that 9 nm could be the threshold $h_{ref}$ for these substrates, below which the interactions between polymer chains and water droplets are inadequate to adhere the droplets at temperatures below LCST. The temperature responsiveness of substrates coated with 50 : 1, 55 : 1 and 60 : 1 PFOTS : poly(MEO$_2$MA-*co*-OEGMA) with $h_{ref} \approx 9$ nm was investigated next.

Substrates coated with 50 : 1 PFOTS : poly(MEO$_2$MA-*co*-OEGMA) ($h_{ref} \approx 9$ nm) did not exhibit temperature-responsive adhesion in water-in-decane emulsions, as shown in Fig. 7a. However, responsiveness was observed for substrates coated with 55 : 1 and 60 : 1 PFOTS : poly(MEO$_2$MA-*co*-OEGMA) in which the surface adhesion could be switched between RT and ~60 °C (Fig. 7b and c). The fact that substrates were completely non-adhesive in the absence of polymer (Fig. 7d) strongly indicates the surface adhesiveness was primarily induced by the polymer chains grafted on the surfaces. At RT (below LCST), when water droplets were in contact with surfaces coated with 55 : 1 and 60 : 1 PFOTS : poly(MEO$_2$MA-*co*-OEGMA) ratios, the interactions between water molecules and the polymer polar ether groups resulted in the adhesion of water droplets on the surfaces. At ~60 °C (above LCST), the intramolecular interactions between apolar carbon–carbon segments within the polymer chains became predominant and the polymer chains no longer anchored the droplets to the surface. As a result, the adhesive force decreased, leading to non-adhesive surfaces. Temperature-responsive adhesion of water droplets on the coated substrates was reproducible over three repeating cycles, demonstrating the stability of the surface coatings at ~60 °C. We demonstrated that responsive adhesion can also be achieved using another temperature-responsive polymer polyNIPAM with a LCST of ~32 °C[26,27] (55 : 1 PFOTS : polyNIPAM) (Fig. 7f).

As shown in Fig. 7e, substrates coated with 100% poly(MEO$_2$MA-*co*-OEGMA) brushes ($h_{ref} \approx 9$ nm) did not exhibit temperature-responsive adhesion. Hence, a key contributory factor to the aforementioned temperature responsiveness obtained at 55 : 1 and 60 : 1 PFOTS : poly(MEO$_2$MA-*co*-OEGMA) ratios could be the "pinning" adhesion due to the non-continuous, phase-segregated polymer coatings (Fig. 4e). The importance of such "archipelago"-like surfaces with discrete domains of polymer brushes on a hydrophobic background to the observed responsive adhesion behaviour was further confirmed by our experiments using gold substrates instead of silicon (ESI, Fig. S3†). Responsive adhesion behaviour was not observed on gold substrates coated with the same copolymer in a similar range of initiator mixture (fluorinated thiol/initiator thiol 40 : 1 to 200 : 1) (ESI, Fig. S4†). These brush-coated gold substrates did not exhibit microscopic phase segregation and homogeneous polymer coatings were observed by AFM throughout the range of thiol mixture investigated (ESI, Fig. S5†). In addition, static contact angles of water in decane at RT were 88–103°, compared to ~140° on silicon substrates with similar coatings.

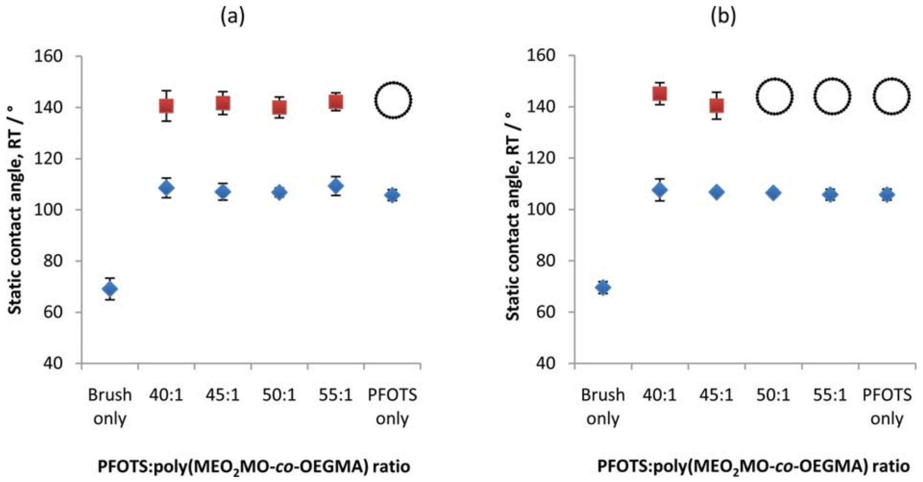

**Fig. 6** Static contact angles of water in air (◆) and water in decane (■) at RT on coated silicon substrates as a function of the PFOTS : poly(MEO$_2$MA-*co*-OEGMA) ratio. (a) $h_{ref} \approx 9$ nm and (b) $h_{ref} \approx 5$ nm. Dotted circles signify that water droplets did not adhere to the surfaces.

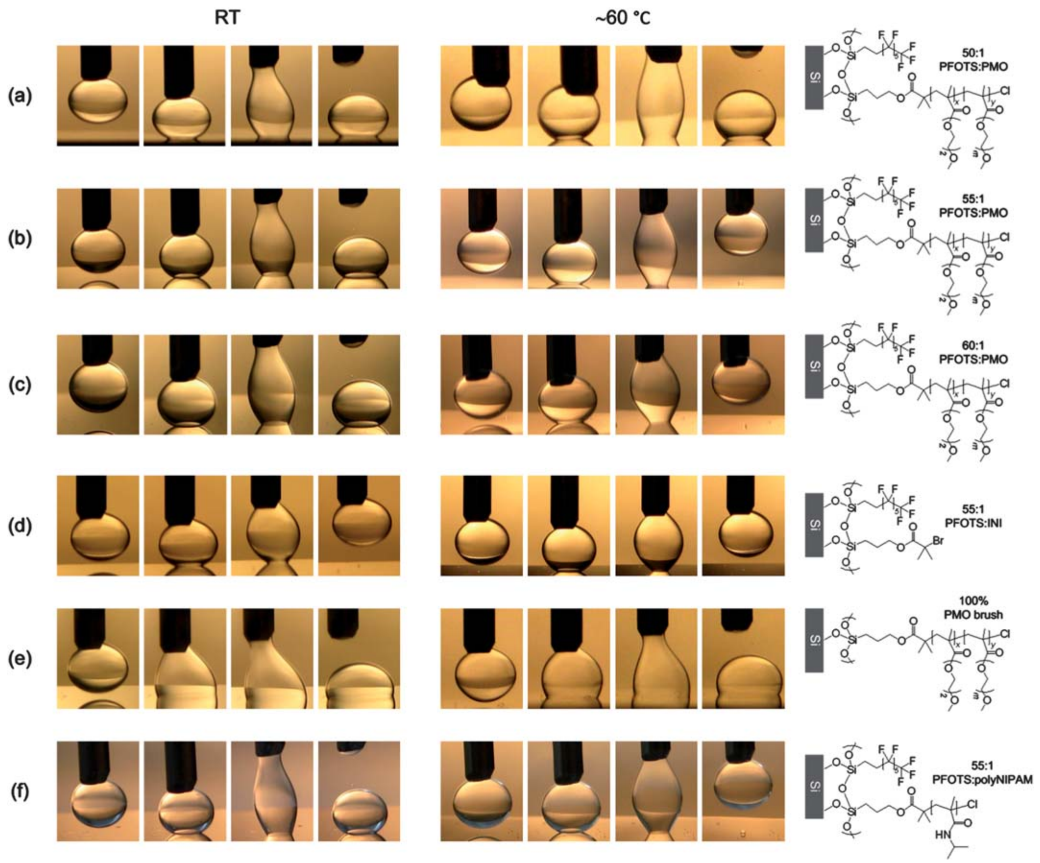

**Fig. 7** Adhesion of water in decane on coated silicon substrates as a function of temperature and various PFOTS : polymer ratios. For (a), (b), (c) and (e), substrates were coated with poly(MEO$_2$MA-*co*-OEGMA) (PMO) ($h_{ref} \approx 9$ nm) at (a) 50 : 1, (b) 55 : 1, (d) 60 : 1 PFOTS : PMO and (e) 100% PMO brush. For (d), substrates were coated with 55 : 1 PFOTS : INI (without polymer). For (f), substrates were coated with polyNIPAM ($h_{ref} \approx 6$ nm) at 55 : 1 PFOTS : polyNIPAM.

Increasing the size of water droplet had negligible effects on the contact angle on silicon surfaces coated with 60 : 1 PFOTS : poly(MEO$_2$MA-*co*-OEGMA) ($h_{ref} \approx 9$ nm) (ESI, Fig. S6a†). Contact angles remained at 138 ± 4° for water droplets with volumes of 1.5–5.0 μL. Responsive adhesion on the surfaces was observed for 1.5 μL and 3.5 μL droplets, as shown in Fig. S6b†. As expected from increasing the droplet size, water droplets with a larger volume (5.0 μL) did not detach from the surfaces at ~60 °C. On the other hand, water droplets with a smaller volume (0.7 μL) did not adhere to the surfaces even at RT, most probably because the pulling force at the needle tip was much stronger than the adhesive force on the surfaces. Hence, the surface chemistry should be modified to match specific applications requiring a given size of droplets.

## pH-responsive adhesive hydrophobic surfaces in water-in-oil emulsions

Silicon substrates coated with INI and/or PFOTS were also used to generate pH-responsive adhesive surfaces in water-in-oil emulsions. PolyDMAEMA with a p$K_a$ at around 7.0[28] was used as the model pH-responsive polymer. Modified substrates were grafted with polyDMAEMA brushes ($h_{ref} \approx 9$ nm) and their pH-responsiveness in water-in-decane emulsions was studied using HCl (pH ≈ 2), NaHCO$_3$ (pH ≈ 8) and NaOH (pH ≈ 12) at the same ionic strength (10 mM).

Analogous to the aforementioned temperature-responsive adhesive surfaces, pH-responsive adhesion in water-in-decane emulsions was observed on surfaces coated with phase-segregated self-assembled layers at 60 : 1 PFOTS : polyDMAEMA ($h_{ref} \approx 9$ nm) (Fig. 8a). Water droplets with pH ≈ 2 stuck to the coated surfaces whereas water droplets with pH ~8 and ~12 could be removed from the surfaces. As the acidic water droplet came into contact with the coated surface, polyDMAEMA became cationic, swelled and turned more hydrophilic, thus giving rise to the surface adhesiveness. For substrates coated with 100% polyDMAEMA brushes ($h_{ref} \approx 9$ nm) (Fig. 8b), water droplets were retained on the surfaces in all cases regardless of pH. This result again implies the importance of phase-separated polymer coatings on responsive adhesion. In agreement with the previous results, substrates coated with 60 : 1 PFOTS : INI without polymer (Fig. 8c) were not adhesive, again suggesting that polymer chains attributed to the responsive adhesion of the substrates. The small residual alkaline water droplets (NaHCO$_3$ 10 mM and NaOH 10 mM) observed on both responsive surfaces (60 : 1 PFOTS : polyDMAEMA) and non-responsive surfaces (100% PFOTS and 60 : 1 PFOTS : INI without polymer) could be attributed to the effects of ionic strength of the droplets on the surfaces.

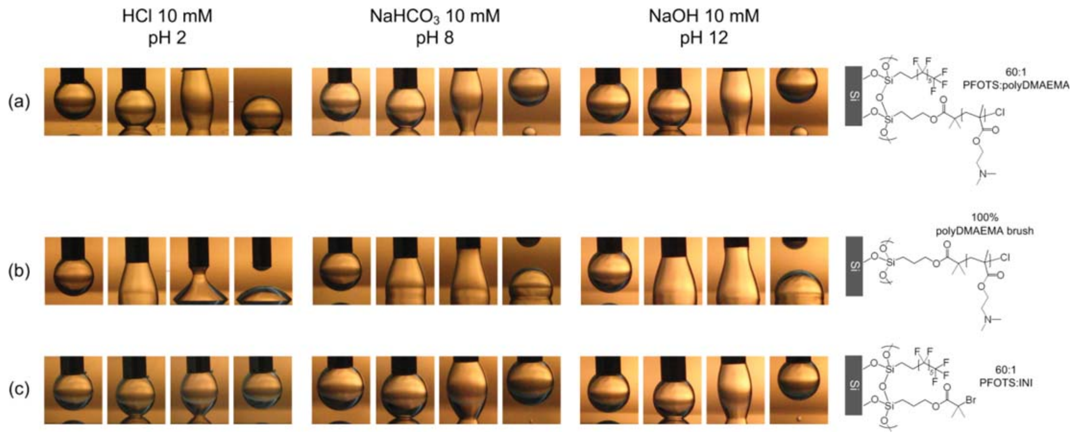

**Fig. 8** Adhesion of water in decane on coated silicon substrates as a function of pH. Substrates were coated with polyDMAEMA ($h_{\mathrm{ref}} \approx 9$ nm) at (a) 60 : 1 PFOTS : polyDMAEMA, (b) 100% polyDMAEMA brush and (c) 60 : 1 PFOTS : INI (without polymer).

## Conclusions

In summary, we fabricated responsive adhesive surfaces *via* a combination of self-assembly and polymer brush growth, using smooth silicon wafer surfaces. The initiator dilution ratio and polymer chain length were two important parameters that allowed us to control responsive adhesion to the surfaces. We demonstrated that the adhesion of water droplets at solid/oil interfaces could be influenced by external signals such as temperature and pH. We believe that the approach described could be applied to a broad range of surfaces with various geometries including glass capillaries, and could ultimately lead to a number of potential applications such as miniature reactors, concentration of minute chemical constituents, and control of droplets in microfluidic devices.

## Acknowledgements

We thank Prof. Feng Zhou (Lanzhou Institute of Chemical Physics) for advice on non-adhesive surfaces. K.Y.T. is grateful to Schlumberger for financial support.

## References

1 R. E. Johnson, Jr and R. H. Dettre, *J. Phys. Chem.*, 1964, **68**, 1744–1750.
2 J. F. Joanny and P. G. De Gennes, *J. Chem. Phys.*, 1984, **81**, 552–562.
3 H. Kusumaatmaja and J. M. Yeomans, *Langmuir*, 2007, **23**, 6019–6032.
4 G. McHale, N. J. Shirtcliffe and M. I. Newton, *Langmuir*, 2004, **20**, 10146–10149.
5 K. Liu, X. Yao and L. Jiang, *Chem. Soc. Rev.*, 2010, **39**, 3240–3255.
6 X. Feng and L. Jiang, *Adv. Mater.*, 2006, **18**, 3063–3078.
7 L. Feng, Y. Zhang, J. Xi, Y. Zhu, N. Wang, F. Xia and L. Jiang, *Langmuir*, 2008, **24**, 4114–4119.
8 L. F. Boesel, C. Cremer, E. Arzt and A. D. Campo, *Adv. Mater.*, 2010, **22**, 2125–2137.
9 M. Liu and L. Jiang, *Adv. Funct. Mater.*, 2010, **20**, 3753–3764.
10 S. Reddy, E. Arzt and A. del Campo, *Adv. Mater.*, 2007, **19**, 3833–3837.
11 X. Zhu, Z. Zhang, X. Men, J. Yang and X. Xu, *Appl. Surf. Sci.*, 2010, **256**, 7619–7622.
12 D. Wang, Y. Liu, X. Liu, F. Zhou, W. Liu and Q. Xue, *Chem. Commun.*, 2009, 7018–7020.
13 D. Wang, X. Wang, X. Liu and F. Zhou, *J. Phys. Chem. C*, 2010, **114**, 9938–9944.
14 C. Li, R. Guo, X. Jiang, S. Hu, L. Li, X. Cao, H. Yang, Y. Song, Y. Ma and L. Jiang, *Adv. Mater.*, 2009, **21**, 4254–4258.
15 X. Liu, Q. Ye, B. Yu, Y. Liang, W. Liu and F. Zhou, *Langmuir*, 2010, **26**, 12377–12382.
16 X. Liu, Q. Ye, X. Song, Y. Zhu, X. Cao, Y. Liang and F. Zhou, *Soft Matter*, 2011, **7**, 515–523.
17 M. Liu, S. Wang, Z. Wei, Y. Song and L. Jiang, *Adv. Mater.*, 2009, **21**, 665–669.
18 L. Chen, M. Liu, L. Lin, T. Zhang, J. Ma, Y. Song and L. Jiang, *Soft Matter*, 2010, **6**, 2708–2712.
19 A. M. Jonas, K. Glinel, R. Oren, B. Nysten and W. T. S. Huck, *Macromolecules*, 2007, **40**, 4403–4405.
20 K. N. Plunkett, X. Zhu, J. S. Moore and D. E. Leckband, *Langmuir*, 2006, **22**, 4259–4266.
21 D. M. Jones, A. A. Brown and W. T. S. Huck, *Langmuir*, 2002, **18**, 1265–1269.
22 F. Fan, C. Maldarelli and A. Couzis, *Langmuir*, 2003, **19**, 3254–3265.
23 J. F. Lutz and A. Hoth, *Macromolecules*, 2006, **39**, 893–896.
24 J. F. Lutz, *J. Polym.Sci., Part A: Polym. Chem.*, 2008, **46**, 3459–3470.
25 A. M. Jonas, Z. J. Hu, K. Glinel and W. T. S. Huck, *Nano Lett.*, 2008, **8**, 3819–3824.
26 J. F. Lutz, Ö. Akdemir and A. Hoth, *J. Am. Chem. Soc.*, 2006, **128**, 13046–13047.
27 D. M. Jones, J. R. Smith, W. T. S. Huck and C. Alexander, *Adv. Mater.*, 2002, **14**, 1130–1134.
28 M. Zhang, L. Liu, H. Zhao, Y. Yang, G. Fu and B. He, *J. Colloid Interface Sci.*, 2006, **301**, 85–91.